IEEE Access
Multidisciplinary | Rapid Review | Open Access Journal

Received May 31, 2019, accepted June 19, 2019, date of publication July 4, 2019, date of current version July 24, 2019.

Digital Object Identifier 10.1109/ACCESS.2019.2926923

Interference Hypergraph-Based 3D Matching Resource Allocation Protocol for NOMA-V2X Networks

BAOJI WANG[1,2,3], RONGQING ZHANG[2,3], (Member, IEEE), CHEN CHEN[1], (Senior Member, IEEE), XIANG CHENG[1], (Senior Member, IEEE), LIUQING YANG[3,4], (Fellow, IEEE), AND YE JIN[1]

[1]State Key Laboratory of Advanced Optical Communication Systems and Networks, School of Electronics Engineering and Computer Science, Peking University, Beijing 100871, China
[2]School of Software Engineering, Tongji University, Shanghai 201804, China
[3]Shandong Provincial Key Lab of Wireless Communication Technologies, Shandong 250100, China
[4]Department of Electrical and Computer Engineering, Colorado State University, Fort Collins, CO 80523, USA

Corresponding author: Rongqing Zhang (rongqingz@tongji.edu.cn)

This work was supported in part by the National Key Research and Development Project under Grant 2017YFE0121400 and Grant 2017YFE0119300, in part by the National Science and Technology Major Project under Grant 2018ZX03001031, in part by the Major Project from Beijing Municipal Science and Technology Commission under Grant Z181100003218007, in part by the National Natural Science Foundation of China under Grant 61622101 and Grant 61571020, and in part by the Open Research Fund from the Shandong Provincial Key Lab of Wireless Communication Technologies under Grant SDKLWCT-2019-02.

ABSTRACT Vehicle-to-everything (V2X) communications are regarded as the key technology in future vehicular networks due to its ability in providing efficient and reliable massive connections, improving traffic efficiency and safety, and supporting in-vehicle entertainment and working. Recently, non-orthogonal multiple access (NOMA), as a promising solution in the fifth-generation (5G) mobile communication systems, has drawn much attention because it can significantly improve the network throughput and lower the accessing and transmission latency to meet the quality-of-service (QoS) requirements of many 5G-enabled applications. Noticing these, in this paper, we consider a device-to-device (D2D)-enhanced V2X network, in which NOMA is introduced to increase the capacity. In our studied NOMA-V2X system, except for the NOMA-based intra-group resource reuse, the D2D-enabled resource sharing based on spatial reuse among all the V2X communication groups is also permitted through centralized resource management, leading to a significantly improved network performance but a more complicated and challenging interference scenario. In order to efficiently manage the interference and allocate the resource in the NOMA-V2X network, we create a weighted 3-partite interference hypergraph (IHG) to imitate the complex interference environment in our studied scenario. Then, with the help of this hypergraph, we make another step to put forward an IHG-based 3-dimensional matching (IHG-3DM) resource allocation protocol with a greedy 3DM algorithm and an iterative 3DM algorithm. As a consequence, the network throughput is significantly improved with the help of our proposed IHG-3DM resource allocation protocol for the investigated NOMA-integrated V2X communications, which is verified by the simulation results.

INDEX TERMS V2X, NOMA, hypergraph, 3D matching, resource allocation.

I. INTRODUCTION

In recent years, the explosive growth of vehicles and heavy information demands have introduced vehicles into communication networks, and made the demand for communication services in vehicles increase. The newly emerging vehicular communication networks (VCN) has become a research and industrial, since it promotes the development of intelligence and cyberized vehicles. The VCN applications in the fifth generation (5G) mobile communication systems have ever-increasing quality of service (QoS) requirements of ultra-high reliability vehicular communications [1], to make VCN safer, smarter and more efficient. By enabling vehicles to exchange information with other vehicles

The associate editor coordinating the review of this manuscript and approving it for publication was Fuhui Zhou.

(i.e., vehicle-to-vehicle, V2V), infrastructures (i.e., vehicle-to-infrastructure, V2I) and cloud (i.e., vehicle-to-cloud, V2C), vehicle-to-everything (V2X) communications can combine many different scenarios to meet different service requirements, including modern intelligent transportation [1]–[3]. V2X communications can be well compatible with the existing road traffic system and communication system, and maximize people's travel efficiency and communication efficiency under effective management [4], [5].

In all the applications of VCN, the vehicle ad-hoc network (VANET) enables communication in V2V during vehicle movement, as well as in V2I at low speed or at rest. Some unfavorable factors, including narrow bandwidth, high mobility, and high node density, have brought great challenges to the design of VANET transmission control protocol. But at the same time, the channel state information (CSI) and vehicle location can be obtained easily in VANET, which is of great significance to design efficient and reliable transmission control protocols [6], [7]. In 2010, the IEEE 802.11p was proposed to form the basic protocol framework for vehicular wireless communications. The IEEE 802.11p has extended the traditional wireless short-range network technology and made a number of specific improvements for vehicular communications, including more advanced hotspot handoff schemes, better support for new communication environment, improved the efficiency of communications, enhanced the user experience, etc. IEEE 802.11p can also reduce the costs of deployment, increase bandwidth, and collect traffic information whenever necessary [8].

In order to meet the growing QoS requirements and the increasing amount of communication data traffic, device-to-device (D2D) communications has been considered to be an effective way of cellular data offloading [9]. D2D communications can increase the cell capacity and spectral efficiency on condition that the interference generated by all the communication links can be managed through effective wireless resource allocation scheme [10]. D2D allows resource allocation under the control of the base station (BS) as well as information interaction without the network infrastructure, which makes it more flexible compared with other pass-through technologies that do not rely on the basic network facilities. Many studies have conducted remarkable research on D2D applications. In [11], by optimizing transmit power and allocating resources effectively, the authors maximized the sum rate of hybrid mode D2D communication system. They studied the channel allocation schemes for D2D links and the optimal power allocation schemes for different modes, thus the overall network sum rate has been greatly improved under the predetermined objective. This study pointed out that mixed mode D2D can help improve the performance of heterogeneous D2D networks. In addition, centralized control of the underlying system of D2D can achieve more efficient and effective deployment of the whole network resources. In [12], the authors studied the possibility of running V2V connections when coexisting with V2I links in the D2D underlay mode, based on the characteristics of the D2D communications and the nature of the vehicular networks. Several improvement schemes for vehicles, including interference control mechanism, predictive resource allocation method and road side unit (RSU) cooperative scheduling method, have been proposed to improve the overall system performance in the intelligent transportation systems (ITS). And it has also indicated that D2D for ITS was still a challenging area, waiting for innovative and practical solutions.

Power domain non-orthogonal multiple access (NOMA) is a promising key multiple access technology in 5G to improve the spectral efficiency significantly, meet the increasing demand in mobile data traffic, and lower the latency compared with traditional orthogonal multiple access (OMA) including frequency division multiplexing (FDM), time division multiplexing (TDM) and code division multiple (CDM) [13], [14]. Whereas orthogonal frequency division multiplexing (OFDM) is the most basic technology of long term evolution (LTE) physical layer. NOMA is the technology that combines successive interference cancellation (SIC) of 3rd-generation (3G) systems and OFDM of 4th-generation (4G) systems. NOMA overcomes the near-far effect problem in 3G systems, as well as solves the co-channel interference problem in 4G systems. Unlike the previous OMA, NOMA uses non-orthogonal power domain to differentiate users, so that the data between users can be transmitted in the same time slot and at the same frequency [15], [16]. OFDM subchannel can still be used as the smallest unit of NOMA, maintaining orthogonality and interference free between subchannels. The corresponding power of each subchannel is shared by multiple users, resulting in multiple access interference (MAI). Therefore, NOMA uses SIC to detect and eliminate multi-user interference at the receiver to ensure the quality of communication.

In recent years, it has become popular to adopt NOMA in vehicular networks. In [17], the authors studied the latent capacity for NOMA in V2X scenario, as well as the difficulty in the next generation communications. In [18], the key issues of interference management and handover in NOMA-enabled 5G vehicular communication systems were studied. A layered power control scheme was proposed to perform joint optimization of cell association and power control to improve the spectral efficiency of the NOMA-enabled 5G vehicular communication system, as well as to adapt to the traffic load conditions and the high mobility. And the authors in [19] studied the power allocation problem for NOMA-enabled heterogeneous vehicular communications with imperfect channel estimation. The effect of channel estimation error caused by high mobility in vehicular communications on achieving effective power allocation and link reliability was demonstrated, and then an improved scheme was proposed. Recently, a spatial-reuse permitted NOMA-V2X network was proposed in [20] resulting in a serious interference environment, and thus the authors constructed an interference hypergraph to deal with the problem. However, the interference model in [20] only considered the conditions that whether the interference exceeded a fixed

threshold or not, and ignored the influence of the interference level, which cannot reflect the real interference environment. Therefore, the effect of the performance optimization for NOMA-V2X networks based on resource-sharing has been limited. At present, the issues of resource allocation and interference management in vehicular communication scenarios with NOMA applied are still need to be solved efficiently.

Recently, graph theory has been widely used in wireless resource scheduling [21], and has achieved good performance. Therefore, it may provide a reliable solution for the scenarios studied in this paper by applying graph theory. In order to solve the resource sharing problem in vehicular networks including both V2V and V2I communication links and achieve a good performance in terms of the sum rate, the authors in [22] proposed two interference graph-based resource-sharing schemes. By constructing an interference-aware graph in vehicular networks, the relationships between the communication links can be expressed clearly, and thus it makes the resource allocation problem easier to be solved efficiently.

In this paper, we investigate the resource allocation problem in NOMA-V2X networks, where both NOMA and spatial reuse-based resource sharing for V2X communications are coexisting under the control of the BS or RSU [20]. Then, we create a weighted 3-partite interference hypergraph (IHG) to imitate the complex interference environment in our studied scenario. Then, with the help of this 3-partite hypergraph, we make another step to put forward a 3-dimensional matching (3DM) resource allocation protocol including a greedy 3DM algorithm and an iterative 3DM algorithm to solve the resource block (RB) allocation problem, resulting in effective RB allocation with acceptable computational complexity. As a consequence, the network throughput is significantly improved with the help of our proposed IHG-3DM protocol for the investigated NOMA-V2X communications, which is verified by the simulation results. The main contributions of this paper are summarized as follows.

- In order to meet the QoS requirements of future 5G-enabled vehicular applications, this paper proposes to integrate the NOMA techniques and D2D-enabled V2X communications to form a novel architecture for 5G-enabled vehicular networks, namely NOMA-V2X, which can significantly improve the network performance. In the NOMA-V2X architecture, three main types of communication groups co-exist, i.e., the V2I group, the multi-V2V group, and the uni-V2V group. Different communication groups can share the spectrum resources through D2D underlaying based spatial reuse, while NOMA is employed in both V2I and multi-V2V groups to increase the intra-group transmission efficiency. The introduced NOMA-V2X architecture can sufficiently exploit both the advantages of NOMA and spatial reuse in improving the spectrum efficiency.
- Although the NOMA-V2X architecture has the potential to obviously improve the network throughput, it is very challenging for the interference control and resource allocation problem in such a scenario with complicated and dynamic interference relationships among communication links. To efficiently solve the resource allocation problem in our studied NOMA-V2X systems, we create a weighted 3-partite interference hypergraph to imitate the complex interference environment and the heterogeneous relationships among all the communication groups. In the 3-partite hypergraph, the vertices represent the communication groups (i.e., multi-V2V, uni-V2V, and V2I), the hyperedges represent the interference among communication groups, and the hyperedge weights denote the achieved throughput.
- In addition, we further establish a weighted interference hypergraph-based 3-dimensional matching (IHG-3DM) resource allocation protocol, which can achieve effective RB allocation with acceptable computational complexity. In the proposed protocol, two RB allocation algorithms, that is, the iterative 3DM algorithm and the greedy 3DM algorithm are further provided. The greedy 3DM algorithm achieves suboptimal network performance with very low complexity, whereas the iterative 3DM algorithm can lead to much better network performance with an acceptable increase in the computational complexity.

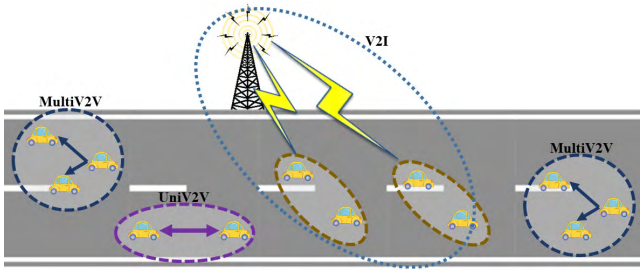

FIGURE 1. An illustrated NOMA-integrated V2X network.

The remainder of this paper is organized as follows. In Section II, we present the system model of the investigated NOMA-integrated V2X scenario and analyze the corresponding objective of this paper. Section III gives the detailed description of the 3-partite hypergraph construction and proposes the IHG-3DM resource allocation protocol including an iterative 3DM algorithm and a greedy 3DM algorithm. In Section IV, the simulation methods, details and results are introduced and evaluated. We conclude our paper in Section V.

II. SYSTEM MODEL AND PROBLEM FORMULATION

A. SYSTEM DESCRIPTION

As illustrated in Fig. 1, there are three types of communication groups in our investigated NOMA-V2X communication scenario [20]. The multi-V2V communication groups are denoted by $\mathcal{M} = \{1, 2, \cdots, M\}$. The uni-V2V communication groups are denoted by $\mathcal{U} = \{1, 2, \cdots, U\}$. And the downlink V2I communication groups are denoted by $\mathcal{V} = \{1, 2, \cdots, V\}$. In our studied NOMA-V2X system, multi-V2V and downlink V2I communication groups apply

NOMA techniques to improve the spectral efficiency. In addition, different communication groups are permitted to reuse the same RB when the QoS guaranteed through effective interference management. As for multi-V2V communications, there is one lead vehicle behaving as the transmitter and broadcasting the superposed messages to all the other vehicles by exploiting NOMA techniques within the same group. The two vehicles in each uni-V2V communication group can exchange information with each other as a D2D underlay to other communication groups. As for V2I communications, the RSU transmits the superposed signals with NOMA techniques to all the vehicles contained in the same NOMA group. OFDM is applied in our investigated NOMA-V2X scenario, where the set of RBs is denoted by $\mathcal{R} = \{1, 2, \cdots, R\}$. Although the applied NOMA technique and the resource sharing mode may bring significant improvement in network spectral efficiency, they will meanwhile make the interference scenario in NOMA-V2X networks more complicated and severer. Hence, whether the caused interference can be effectively limited determines the performance achieved by the investigated NOMA-V2X network. In our investigated NOMA-V2X scenario, we mainly consider two kinds of interference. The interference caused by the superposition signals with NOMA namely intra-group interference. The interference caused by the resource reusing among different communication groups namely inter-group interference. In the studied NOMA-V2X network, multi-V2V and downlink V2I communications suffer two kinds of interference at the same time, whereas the uni-V2V communication group only suffers the inter-group interference. Therefore, in order to achieve the potential benefits of NOMA-V2X in vehicular networks, our main objective in this paper is to control the interference and allocate the resource among different communication links through low-complexity protocol, and finally improve the network throughput.

B. SUCCESSIVE INTERFERENCE CANCELLATION

With NOMA, the introduction of overlapped information at the transmitter may bring higher spectral efficiency, but it also causes the MAI problem. In the literature, SIC has been regarded as a promising way to eliminate the MAI [23], [24]. In NOMA systems, SIC can be also implemented at the receivers for multi-user detection. The basic idea of SIC is to adopt a step-by-step interference eliminating strategy, and the messages are detected one by one in the received signal. After the amplitude recovery, the MAI generated by one user's signal is subtracted from the received signal. Then, the receiver detects the messages again in the remaining signals and subtracts the MAI generated by another user's signal. The receiver will repeat this operation until all the MAIs are eliminated. The order of the interference elimination is decided in view of the power of the users' signals. The BS allocates different signal power to different users through power multiplexing techniques to distinguish the users and obtain the maximum system performance gain.

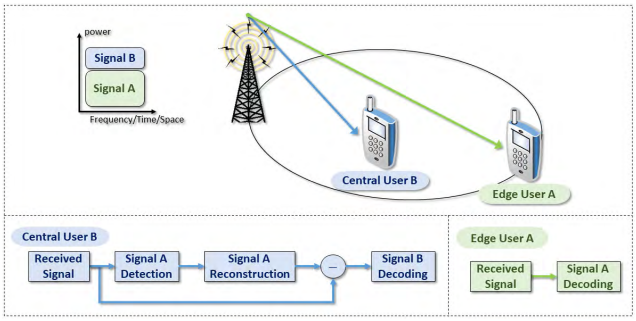

FIGURE 2. NOMA with successive interference cancellation.

In a typical NOMA system, as shown in Fig. 2, the BS sends the superimposed messages to the users with different power. To make sure the user with a worse channel condition (i.e., user A) can decode its own message immediately by ignoring the other users' messages as the noise, the BS needs to allocate more transmit power to user A. Whereas the user with a better channel condition (i.e., user B) is allocated with less transmit power, and thus user B has to first decode user A's message, and then subtract it from its received signal to get user B's own message.

C. PROBLEM FORMULATION

Generally, the number of vehicles included in one NOMA group is random. A fixed number of vehicles in one NOMA group can limit the multi-user interference within the NOMA group and reduce the computational complexity. Without loss of generality, we assume that there are Q vehicles in each multi-V2V communication group. At the same time, we assume that there are $Q-1$ vehicles in each V2I communication group. Denote $\mathcal{Q} = \{1, 2, \cdots, Q\}$ and $\mathcal{Q}^- = \{1, 2, \cdots, Q-1\}$. In a multi-V2V group $m \in \mathcal{M}$, m_1 transmits the NOMA superposition signals, whereas m_i ($i \neq 1, i \in \mathcal{Q}$) receives the signals. In a V2I communication group $v \in \mathcal{V}$, $v_j (j \in \mathcal{Q}^-)$ receives the NOMA superposition signal from the RSU. As for uni-V2V group $u \in \mathcal{U}$, u_1 transmits signals to the receiver u_2. Meanwhile, let $m' \in \mathcal{M}$ denotes another multi-V2V group different from m, and thus m'_1 will transmit the NOMA superposition signals to the receivers m'_i ($i \neq 1, i \in \mathcal{Q}$). Similarly, let $u' \in \mathcal{U}$ denotes another uni-V2V group different from u, then, u'_1 will transmit the NOMA superposition signals to the receiver u'_2. The notations in this paper are set as follows:

- *Channel coefficient*: $\mathcal{H}_{m_i}$, $\mathcal{H}^{m'}_{m_i}$, $\mathcal{H}^{u}_{m_i}$, and $\mathcal{H}^{v}_{m_i}$ denote the channel gains from m_1 to m_i ($i \neq 1$), m'_1 to m_i ($i \neq 1$), u_1 to m_i ($i \neq 1$), and RSU to m_i ($i \neq 1$), respectively; $\mathcal{H}_{v_j}$, $\mathcal{H}^{m}_{v_j}$, and $\mathcal{H}^{u}_{v_j}$ denote the channel gains from RSU to v_j, m_1 to v_j, and u_1 to v_j, respectively; $\mathcal{H}_{u_2}$, $\mathcal{H}^{m}_{u_2}$, $\mathcal{H}^{u'}_{u_2}$, and $\mathcal{H}^{v}_{u_2}$ denote the channel gains from u_1 to u_2, m_1 to u_2, u'_1 to u_2, and RSU to u_2, respectively;
- *Interference*: $I^{intra}_{m_i}$ denotes the intra-group interference at m_i ($i \neq 1$); $I^{m'}_{m_i}$, $I^{u}_{m_i}$, and $I^{v}_{m_i}$ denote the interferences from m'_1 to m_i ($i \neq 1$), u_1 to m_i ($i \neq 1$), and RSU to m_i ($i \neq 1$), respectively; $I^{intra}_{v_j}$ denotes the intra-group

interference at v_j; $I_{v_j}^{m}$ and $I_{v_j}^{u}$ denote the interferences from m_1 to v_j and u_1 to v_j, respectively; $I_{u_2}^{m}$, $I_{u_2}^{u'}$, and $I_{u_2}^{v}$ denote the interferences from m_1 to u_2, u_1' to u_2, and RSU to u_2, respectively.

In NOMA systems, superposition coding is needed at the transmitter to superpose all users' messages together, thus the NOMA receivers need to apply SIC in order to decode their own messages. As the transmitter in a multi-V2V group $m \in \mathcal{M}$, m_1 transmits the superposed messages to the NOMA receivers within the same communication group $m \in \mathcal{M}$ under different transmit power. Therefore, the received signal on RB $r \in \mathcal{R}$ at m_i ($i \neq 1$) can be given as

$$\begin{aligned} y_{m_i} = & \sum_{q\neq 1, q\in\mathcal{Q}} \mathcal{H}_{m_i}\sqrt{a_{m_q}P_m}x_{m_q} + \zeta_{m_i} \\ & + \sum_{u\in\mathcal{U}} \eta_m^u \mathcal{H}_{m_i}^u \sqrt{P_u}x_u + \sum_{v\in\mathcal{V}} \eta_m^v \mathcal{H}_{m_i}^v \sqrt{P_v}x_v \\ & + \sum_{m'\neq m} \eta_m^{m'} \mathcal{H}_{m_i}^{m'} \sqrt{P_m}x_{m'} \end{aligned} \tag{1}$$

where $\boldsymbol{a_m} = \{a_{m_2}, a_{m_3}, \cdots, a_{m_Q}\}$ denote the transmit power allocation coefficients. x_{m_q} and P_m are the transmit signal and transmit power from m_1 to m_i ($i \neq 1, i \in \mathcal{Q}$), respectively. x_u and P_u are the transmit signal and transmit power from u_1 to u_2, respectively. x_v and P_v are the transmit signal and transmit power from the RSU to $v_j (j \in \mathcal{Q}^-)$, respectively. And $x_{m'}$is the transmit signal from m_1' to m_i' ($i \neq 1, i \in \mathcal{Q}$). ζ_{m_i} is the additive white Gaussian noise (AWGN) with the variance σ^2. The RB allocation indicator is denoted by the vector $\boldsymbol{\eta} \in \mathbb{N}$. $\eta_m^{m'} = 1$ when $m \in \mathcal{M}$ and $m' \in \mathcal{M}$ are working through the same RB $r \in \mathcal{R}$ simultaneously, otherwise, $\eta_m^{m'} = 0$.

Therefore, the received signal to interference and noise ratio (SINR) at m_i ($i \neq 1$) can be given as

$$\varphi_{m_i} = \frac{\left|\mathcal{H}_{m_i}\right|^2 P_m a_{m_i}}{I_{m_i}^{intra} + I_{m_i}^{m'} + I_{m_i}^{u} + I_{m_i}^{v} + \sigma^2} \tag{2}$$

Similarly, the received signals at the uni-V2V group u can be given as

$$\begin{aligned} y_{u_2} = & \mathcal{H}_{u_2}\sqrt{P_u}x_u + \sum_{u'\neq u} \eta_u^{u'} \mathcal{H}_{u_2}^{u'} \sqrt{P_u}x_{u'} + \zeta_{u_2} \\ & + \sum_{m\in\mathcal{M}} \eta_u^m \mathcal{H}_{u_2}^m \sqrt{P_m}x_m + \sum_{v\in\mathcal{V}} \eta_u^v \mathcal{H}_{u_2}^v \sqrt{P_v}x_v \end{aligned} \tag{3}$$

where x_u' denotes the transmit signals from u_1'.

The received SINRs at the uni-V2V group u can be given as

$$\varphi_{u_2} = \frac{\left|\mathcal{H}_{u_2}\right|^2 P_u}{I_{u_2}^{u'} + I_{u_2}^{m} + I_{u_2}^{v} + \sigma^2} \tag{4}$$

Analogously, the received signals at the V2I group v can be given as

$$\begin{aligned} y_{v_j} = & \sum_{q\in\mathcal{Q}^-} \mathcal{H}_{v_j}\sqrt{a_{v_q}P_v}x_{v_q} + \sum_{m\in\mathcal{M}} \eta_v^m \mathcal{H}_{v_j}^m \sqrt{P_m}x_m \\ & + \sum_{u\in\mathcal{U}} \eta_v^u \mathcal{H}_{v_j}^u \sqrt{P_u}x_u + \zeta_{v_j} \end{aligned} \tag{5}$$

The received SINRs at the V2I group v can be given as

$$\varphi_{v_j} = \frac{\left|\mathcal{H}_{v_j}\right|^2 P_v a_{v_j}}{I_{v_j}^{intra} + I_{v_j}^{m} + I_{v_j}^{u} + \sigma^2} \tag{6}$$

The ζ_{u_2} in Eq. (3) and the ζ_{v_j} in Eq. (5) are the AWGN with variance σ^2. The vector $\boldsymbol{a_v} = \{a_{v_1}, a_{v_2}, \cdots, a_{v_{Q-1}}\}$ in Eq. (5) is the power allocation coefficients. The interferences appearing in Eq. (2), Eq. (4), and Eq. (6) are:

- *Interference*:

$$I_{m_i}^{*_m} = \sum_{*_m} \eta_m^{*_m} P_{*_m} \left|\mathcal{H}_{m_i}^{*_m}\right|^2, \; I_{v_j}^{*_v} = \sum_{*_v} \eta_v^{*_v} P_{*_v} \left|\mathcal{H}_{v_j}^{*_v}\right|^2$$

$$I_{u_2}^{*_u} = \sum_{*_u} \eta_u^{*_u} P_{*_u} \left|\mathcal{H}_{u_2}^{*_u}\right|^2, \; I_{*_{int}}^{intra} = \sum_{intra} \mathcal{H}_{*_{int}} \left|^2 P_{*_{int}} a_{*_{int}}\right.$$

where $*_m$ can be replaced by m', u, or v, which denote the parameters at multi-V2V group m', uni-V2V group u, or V2I group v, respectively. $*_u$ can be replaced by m, u', or v, which denote the parameters at multi-V2V group m, uni-V2V group u', or V2I group v, respectively. $*_v$ can be replaced by m or u, which denote the parameters at multi-V2V group m or uni-V2V group u, respectively. $*_{intra}$ can be replaced by m_i or v_j, which denote the parameters at multi-V2V group m or V2I group v, respectively. In addition, the $\eta_m^{*_m}$, $\eta_u^{*_u}$, and $\eta_v^{*_v}$ are the RB allocation indicators in the multi-V2V group m, uni-V2V group u, and V2I group v, respectively. And all these indicators have the same meaning as $\eta_m^{m'}$, which is mentioned above, that is,

$$\eta = \begin{cases} 1 & \text{reuse the same RB,} \\ 0 & \text{otherwise.} \end{cases}$$

Then, based on all the formulas above and the Shannon formula, we can get the expression for calculating the sum rate of the whole network, which can be given as

$$\begin{aligned} R_{sum} = & \sum_{m\in\mathcal{M}} \sum_{i\neq 1, i\in\mathcal{Q}} \left\{BW_m \cdot \log_2\left(1+\varphi_{m_i}\right)\right\} \\ & + \sum_{v\in\mathcal{V}} \sum_{j\in\mathcal{Q}^-} \left\{BW_v \cdot \log_2\left(1+\varphi_{v_j}\right)\right\} \\ & + \sum_{u\in\mathcal{U}} \left\{BW_u \cdot \log_2\left(1+\varphi_{u_2}\right)\right\} \end{aligned} \tag{7}$$

Based on the above analysis, we first fix the power allocation coefficients, so that the RB allocation problem for the NOMA-V2X system can be expressed as

$$\max \quad R_{sum}(\boldsymbol{\eta}) \tag{8a}$$

$$\text{s.t.} \quad \varphi_{m_i}, \varphi_{v_j}, \varphi_{u_2} \geq \varphi_0, \quad \forall m \in \mathcal{M}, v \in \mathcal{V}, u \in \mathcal{U} \tag{8b}$$

$$\sum_{r\in\mathcal{R}} \boldsymbol{\eta} \leq 1, \quad \forall m, u, v \tag{8c}$$

$$\sum_{m,u,v} \boldsymbol{\eta} \leq q_{max}, \quad \forall r \in \mathcal{R} \tag{8d}$$

where Eq. (8b) ensures that the received SINR at each vehicle is greater than the demodulation threshold. Eq. (8c) limits the number of RB that can be allocated to each communication

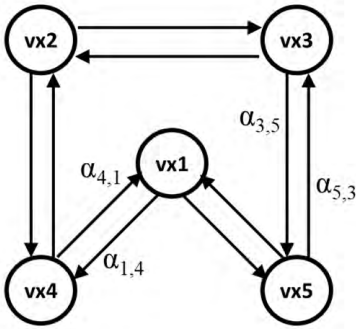

FIGURE 3. An illustration of a weighted graph.

group to 1. Eq. (8d) restricts the number of communication groups that can reuse the same RB at the same time, so as to ensure that each communication group in the same RB can obtain a required QoS.

III. IHG-3DM RESOURCE ALLOCATION PROTOCOL

In this section, we utilize the weighted 3-partite interference hypergraph to imitate the complex interference environment in our studied NOMA-V2X system. Next, with the help of this 3-partite hypergraph, we make another step to put forward an IHG-3DM RB allocation protocol with two efficient 3DM algorithms, that is, the greedy 3DM algorithm and the iterative 3DM algorithm.

A. HYPERGRAPH CONSTRUCTION

Similar to D2D communications in cellular networks, here in our investigated NOMA-V2X network, both multi-V2V and uni-V2V groups can also behave as an underlay to V2I groups to enhance the network performance. However, the resulted interference relationships become much more complicated than the cellular-D2D scenario. In order to model the complicated interference scenario more efficiently and reduce the resource allocation complexity, multi-V2V and uni-V2V groups are first pre-partitioned based on their mutual interference to form a spatial reuse cluster.

For the group pre-partition, we first divide the multi-V2V and uni-V2V groups into different clusters $\mathcal{C} = \{1, 2, \cdots, C\}$ based on their mutual interference. In order to efficiently calculate the interference value between the groups, we exploit a weighted graph to model the interference relationships among the multi-V2V and uni-V2V groups. We use Fig. 3 to express the connection between multi-V2V/uni-V2V groups and their weights. As illustrated in Fig. 3, each multi-V2V/uni-V2V group is modeled as a vertex while the connected edge weight $\alpha_{k,k'}$ is set to capture the interference level from the k'th vertex's transmitter to the kth vertex's receiver.

Referring to [27], the procedure of the partition algorithm is provided in Algorithm 1. First, we assign each cluster one multi-V2V or uni-V2V in an arbitrary manner. Then, by checking the intra-cluster interference value, we further add each remaining multi-V2V and uni-V2V group to a cluster that resulting in the lowest intra-cluster interference value.

Algorithm 1 Partitioning Algorithm

Input: $\mathcal{M}, \mathcal{U}$.
Arbitrarily assign one vertex to each of the C clusters.
foreach $k \in \{\mathcal{M}, \mathcal{U}\}$ *and not already in any cluster* **do**
  for $n = 1 : C$ **do**
    Calculate the increased intra-cluster interference using $\sum_{k' \in c_n} (\alpha_{k,k'} + \alpha_{k',k})$
  end
  Assign the kth vertex to the n^*th cluster with $n^* = \text{argmin} \sum_{k' \in c_n} (\alpha_{k,k'} + \alpha_{k',k})$
end
Output: Cluster $\mathcal{C}$.

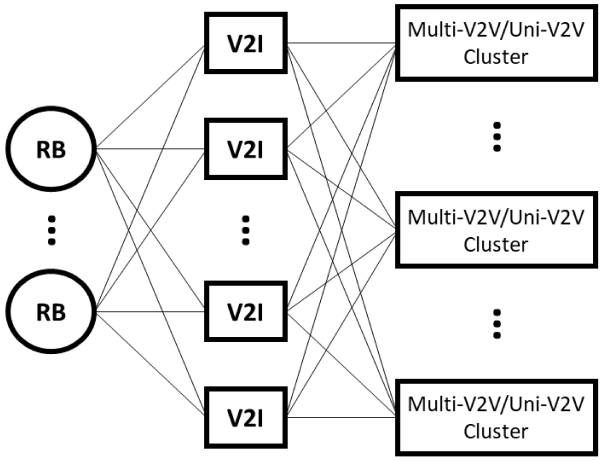

FIGURE 4. An illustration of a weighted 3-partite hypergraph.

After all the multi-V2V/uni-V2V groups are partitioned, the interference environment in the studied NOMA-V2X system can be modeled as a hypergraph. As for a hypergraph, if all the hyperedges have the same number of vertices (like z), the hypergraph is called a z-uniform hypergraph. If the vertices of z-uniform hypergraph can be divided into z disjoint non-empty subsets to make all the vertices of each hyperedge not in the same subset, then the hypergraph is a z-partite hypergraph.

Let $\mathcal{HG} = (\mathcal{HV}, \mathcal{HE})$ be a 3-partite hypergraph, where $\mathcal{HV}$ is the set of vertices representing communication groups or RBs, and $\mathcal{HE}$ is the set of hyperedges representing the matching relationships between vertices. The weight ω for the hyperedge is set to be the sum rate achieved via the denoted RB and communication groups matching. Here, the RB allocation problem in Eq. (8) can be modeled as an effective matching in the weighted 3-partite hypergraph $\mathcal{HG}$ shown in Fig. 4. Note that the number of the clusters C is dynamically set according to the scenario and the number of communication groups. Here for the convenience of constructing the 3-partite hypergraph, we set the number of the clusters equal to that of V2I groups, i.e., $C = V$.

It is worth mentioning that, different V2I groups with the same RSU as the transmitter cannot reuse the same RB at

the same time in the investigated NOMA-V2X network, due to significant co-channel interference without NOMA design crossing different V2I groups. Whereas the V2I groups belonging to different RSUs can still reuse the same RB based on our proposed IHG-3DM RB allocation protocol.

Then, the hypergraph matching problem can be formulated as an integer program:

$$\max \sum_{e\in\mathcal{HE}} \omega(e)t(e) \tag{9a}$$

$$\text{s.t.} \sum_{e\in\delta(v)} t(e) \le 1, \quad \forall v \in \mathcal{HV} \tag{9b}$$

$$t(e) \in \{0, 1\}, \quad \forall e \in \mathcal{HE} \tag{9c}$$

where $\delta(v)$ denotes the set of hyperedges containing vertex v, and let $t(\mathcal{F}) = \sum_{e\in\mathcal{F}} t\{e\}$ denoting a subset of hyperedges $\mathcal{F} \subseteq \mathcal{HE}$.

Therefore, our objective is to find an optimal $t(e)$, which satisfies Eq. (9). Then, we get an independent set $\mathcal{HV}$ so that Eq. (8) is satisfied.

B. IHG-3DM RB ALLOCATION PROTOCOL

In this section, with the help of our created weighted hypergraph, we put forward the IHG-3DM RB allocation protocol. The detailed procedure of the proposed IHG-3DM RB allocation protocol is provided in Fig. 5.

First, the central BS or RSU collects the information of all the vehicles in the current area, including the location information and the communication mode (i.e., multi-V2V, uni-V2V or V2I). Then, the multi-V2V and uni-V2V vehicles are clustered properly to initially limit the intra-group interference through RB sharing and construct the weighted 3-partite hypergraph.

After that, a greedy 3DM algorithm or an iterative 3DM algorithm will be processed to allocate RBs according to different conditions based on the constructed 3-partite hypergraph, resulting in an appropriate matching. Note that the time-varying channel characteristics and the locations of the vehicles will change along with time. Therefore, we need to update the graph/hypergraph and reprocess the corresponding algorithms periodically, ensuring the constructed graph/hypergraph can reflect the current channel state well. The algorithms proposed in the IHG-3DM RB allocation protocol (i.e., the greedy 3DM algorithm and the iterative 3DM algorithm) are described in the following sections.

C. GREEDY 3DM ALGORITHM

The greedy 3DM algorithm can find a suboptimal result of $t(e)$ in a greedy manner with low complexity, in which we search all the vertices to choose an independent set of hyperedges with the highest weight in the 3-partite hypergraph $\mathcal{HG}$ [25]. In the proposed greedy 3DM algorithm, the matching that maximizes the current sum rate is selected at each step. We first sort all the hyperedges in the descending order according to their weights. Then, we select the hyperedge with the maximum weight as part of the output matching sequentially, and skip the hyperedges that intersect

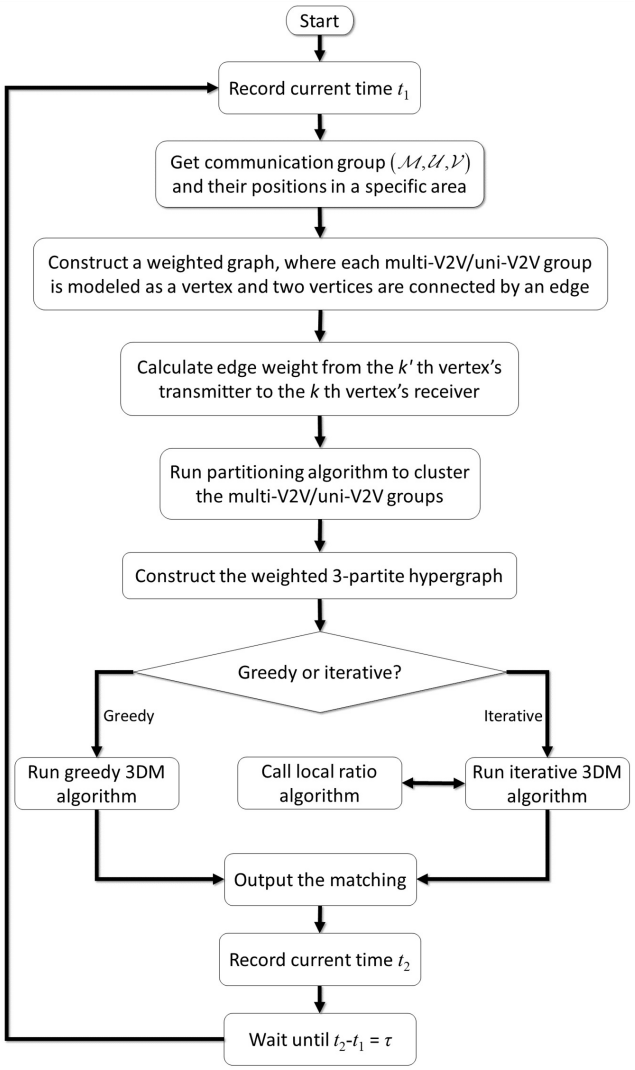

FIGURE 5. Flow diagram of the IHG-3DM RB allocation protocol.

the selected hyperedges. The detailed procedure of the proposed greedy 3DM algorithm is shown in Algorithm 2.

The $N[e]$ in Algorithm 2 denotes the set of hyperedges that intersect the hyperedge e, note that $e \in N[e]$.

The greedy 3DM algorithm is a straightforward but efficient algorithm, which leads to suboptimal solution with very low complexity. During the procedure of the algorithm, each choice simplifies the problem to a smaller sub-problem, which greatly improves its efficiency.

D. ITERATIVE 3DM ALGORITHM

In the proposed greedy 3DM algorithm, after choosing the hyperedge with the maximum weight for each vertex, we ensure that the other vertices in the same hyperedge do not intersect with all the selected hyperedges, which makes the other vertices in this hyperedge lose the possibility of choosing their own maximum-weight hyperedge.

In order to avoid the disadvantages of the greedy 3DM algorithm and make the global result more optimized,

Algorithm 2 Greedy 3DM Algorithm

Input: $\mathcal{HG}, \omega, \mathcal{C}, \mathcal{V}$.
Initialization: $\mathcal{P} \leftarrow \emptyset$.
$\mathcal{HE}_{sort} = \text{sort}(\mathcal{HE}, \text{'descent'})$
for $e \in \mathcal{E}_{sort}$ **do**
  if $N[e] \cap \mathcal{P} = \emptyset$ **then**
    $\mathcal{P} \leftarrow \mathcal{P} \cup e$
  end
end
Output: Matching $\mathcal{P}$.

we further propose an iterative 3DM algorithm referring to [26], [27] for different communication groups in the NOMA-V2X network.

In order to simplify the formulated optimization problem and reduce the computational complexity to find a near-optimal solution, we have the relaxation of the integer program in Eq. (9) as

$$\max \sum_{e \in \mathcal{HE}} \omega(e) t(e) \tag{10a}$$

$$\text{s.t.} \sum_{e \in \delta(v)} t(e) \leq 1, \quad \forall v \in \mathcal{HV} \tag{10b}$$

$$t(e) \geq 0, \quad \forall e \in \mathcal{HE} \tag{10c}$$

Therefore, the objective here is to find a result of $t(e)$ as a basis, which satisfies Eq. (10), and then obtain the final matching in an iterative manner. First, the iterative 3DM algorithm solves a linear programming relaxation and obtains a basic solution, which is used to obtain an integral solution iteratively. Then, it rounds up the large value variables to solve the problem and gets an appropriate matching result. The detailed process of the iterative 3DM algorithm is summarized in Algorithm 3.

Algorithm 3 Iterative 3DM Algorithm

Input: $\mathcal{HG}, \omega, t, \mathcal{C}, \mathcal{V}$.
Initialization: $\mathcal{F} \leftarrow \emptyset$.
while $\mathcal{HE} - \mathcal{F} \neq \emptyset$ **do**
  Find a hyperedge e with $t(N[e] \cap (\mathcal{HE} - \mathcal{F})) \leq 2$
  Set $e_i \leftarrow e$
  Set $\mathcal{F} = \mathcal{F} \cup \{e_i\}$
end
$P \leftarrow$ Local-Ratio($\mathcal{F}, \omega$) using Algorithm 4
Output: Matching $\mathcal{P}$.

In Algorithm 3, the solution t to the linear program Eq. (10) is basic. Some linear programming algorithms, such as simplex algorithm, should be used to obtain a basic solution to the linear program [27].

It is worth mentioning that, the time-varying channel characteristics and the locations of the vehicles will change along with time. But the moving distance of a vehicle is small within time τ (in the magnitude of milliseconds), and the location of a vehicle after a movement in τ on the driveway is highly predictable due to relatively stable movement feature of the vehicles along the road within a short period. Therefore, the proposed IHG-3DM RB allocation protocol can handle the mobility problem easily by updating the hypergraph in a dynamic manner (i.e., periodically in time τ).

Algorithm 4 Local Ratio Algorithm (A Recursive Subroutine)

Input: $\mathcal{F}, \omega$.
Initialization: $\mathcal{F}' = \{e \in \mathcal{F} : \omega(e) > 0\}$.
if $\mathcal{F}' = \emptyset$ **then**
  Return $\emptyset$
end
Choose from $\mathcal{F}'$ the hyperedge e with the smallest index.
Decompose the weight vector $\omega = \omega_1 + \omega_2$ where

$$\omega_1(e') = \begin{cases} \omega(e) & \text{if} \quad e' \in N[e], \\ 0 & \text{otherwise} \end{cases}$$

$\mathcal{P}' \leftarrow$ Local-Ratio($\mathcal{F}', \omega_2$).
if $\mathcal{P}' \cup \{e\}$*is a matching* **then**
  Return $\mathcal{P} := \mathcal{P}' \cup \{e\}$
  else
  Return $\mathcal{P} := \mathcal{P}'$
end
Output: Matching $\mathcal{P}$.

E. COMPLEXITY ANALYSIS

Assume that $|\mathcal{HV}| = \varepsilon$ and $|\mathcal{HE}| = \lambda$. The proposed greedy 3DM algorithm mainly contains a sorting process, and thus the worst-case complexity of the greedy 3DM algorithm is $O(\lambda^2)$.

As for the provided iterative 3DM algorithm, the loop terminates when $\mathcal{HE} - \mathcal{F} = \emptyset$, which means the total number of the iterations is ε. In each iteration, the searching operation has the complexity of $O(\lambda^2 \ log\lambda)$. Whereas the local ratio algorithm given in Algorithm 4 has the complexity of $O(\lambda^2)$, which can be called ε times. Hence, the total complexity of the iterative 3DM algorithm is $O(\varepsilon\lambda^2 \ log\lambda)$.

IV. NUMERICAL RESULTS AND DISCUSSIONS

Our simulation setup considers a 1km×40m 2-way street with one RSU at one side center of the road. We consider an urban micro system [28], and the path loss (PL) is

$$PL(\text{dB}) = 36.7\log_{10}(d) + 22.7 + 26\log_{10}(f_c) \tag{11}$$

where d is the distance between the transmitter and the receiver and f_c is the carrier frequency.

In the simulations, we randomly arrange vehicles in the considered area of the road. For simplicity and without loss of generality, we set $Q = 3$. As described in Section II-C, $Q = 3$ means that each multi-V2V group contains 3 vehicles, and each V2I group contains 2 vehicles. Hence, in the considered area of the road, the total number of the vehicles is set as $(7, 14, \cdots, 70)$. All the other parameters applied in our simulation are summarized in Table 1.

TABLE 1. System parameters.

Parameters	Value
Carrier frequency	2 GHz
Total Bandwidth	20 MHz
RB Bandwidth	100 KHz
RSU's Transmit Power $V \cdot P_v$	24 dBm
Vehicles Transmit Power P_m,P_u	6 dBm
Small-scale Fading	Rayleigh fading
Noise Power Spectral Density	-174 dBm/Hz
Noise Figure	10 dB
Velocity of Vehicles	72km/h $\sim$ 144km/h
Hypergraph Refresh Interval τ	1s
$\boldsymbol{a_m} = \boldsymbol{a_v}$	$(0.4, 0.6)$

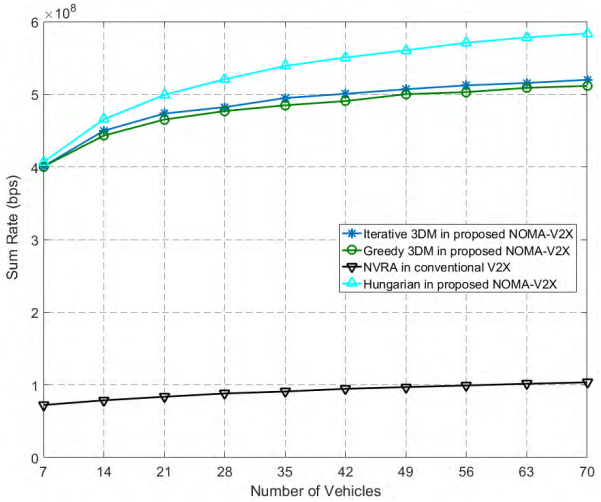

FIGURE 6. Sum rate comparison with different V2X networks.

In order to demonstrate the superiority of our proposed NOMA-V2X network and the IHG-3DM RB allocation protocol, we employ a conventional V2X network as benchmark for performance comparison. Literature [29] presents a basic V2X scenario, including NOMA-based V2I communications and traditional V2V communications. In the V2X network investigated in [29], V2I links can simply reuse the RBs of V2V links to some extent. As shown in Fig. 6, the throughput achieved by our proposed NOMA-V2X network and the IHG-3DM RB allocation protocol is four times that of the conventional V2X network in [29]. Note that NOMA is applied in V2I links in [29], so that the performance of our proposed network and protocol will be more advantageous when compared with the pure V2X network without NOMA.

In Fig. 6, we also compare the performance of Hungarian algorithm [30], [31] in our proposed NOMA-V2X network. Hungarian algorithm is a combinatorial optimization algorithm for solving task assignment problem in polynomial time, e.g. $O(V^3)$, but it cannot be directly applied to the NOMA-V2X network we proposed. Therefore, we need to reduce the dimension of this matching problem. The first step is to partition the multi-V2V and uni-V2V groups into clusters using Hungarian algorithm, similar to the pre-partitioning in our proposed protocol. In the second step, the Hungarian algorithm is applied again to match the V2I links and the

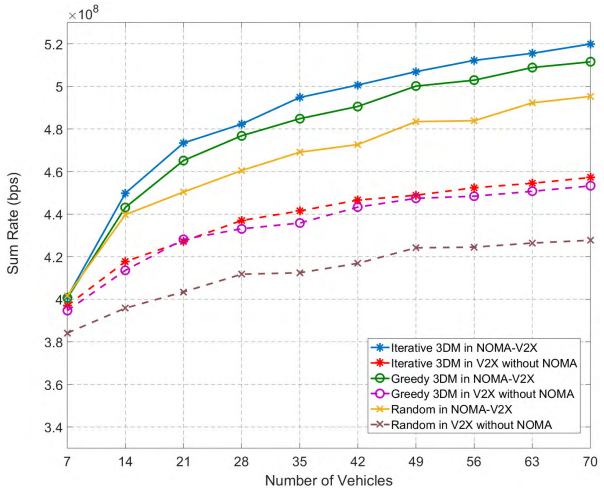

FIGURE 7. Sum rate comparison with different algorithms in our proposed V2X network.

clusters. As we can see in Fig. 6, the performance of our proposed algorithms in the NOMA-V2X network are close to the optimal solution, but with reduced complexity.

As a baseline, we also employ a random RB allocation algorithm based on the constructed 3-partite hypergraph, which randomly selects a disjoint hyperedge as part of the matching until all the vertices are allocated. In the random RB allocation algorithm, all the hyperedges need to be traversed, and a double-level loop is required in order to ensure that the selected hyperedges are disjoint, resulting in a complexity of $O(\lambda^2)$.

In order to further demonstrate the performance improvement of our proposed NOMA-V2X network due to the addition of NOMA, Fig. 7 shows the network sum rate performance comparison among different RB allocation algorithms in both NOMA and non-NOMA scenarios, in which we can see that our proposed IHG-3DM RB allocation protocol with the iterative 3DM algorithm achieves the best network sum rate with an acceptable computational complexity as analyzed in Section III-E. And we can also find that the sum rate increases along with the number of the involved vehicles increasing. However, the increasing rate of the sum rate improvement becomes lower when the number of the vehicles further increases. This is because the NOMA-V2X system we considered contains a lot of influencing factors, and the inter-group interference can have a great impact on the performance of the system. With the number of the vehicles increasing, the number of the communication groups allocated to the same RB also increases, which means the interference relationships among the communication links become more complicated and the introduced interference is higher. Therefore, the corresponding inter-group interference and the spatial reuse gain will reach a relatively stable tradeoff through effective interference management and resource allocation.

It is also shown in Fig. 7 that the scenario without NOMA is used as a basis to highlight the advantages of applying NOMA in V2X communications. For the sake of fairness, we use

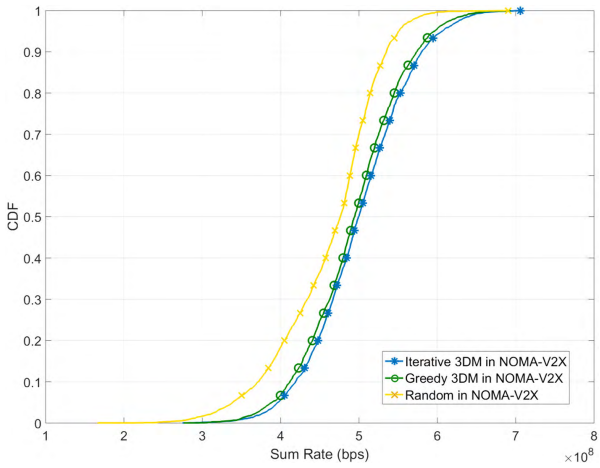

FIGURE 8. Sum rate CDF comparison with different algorithms.

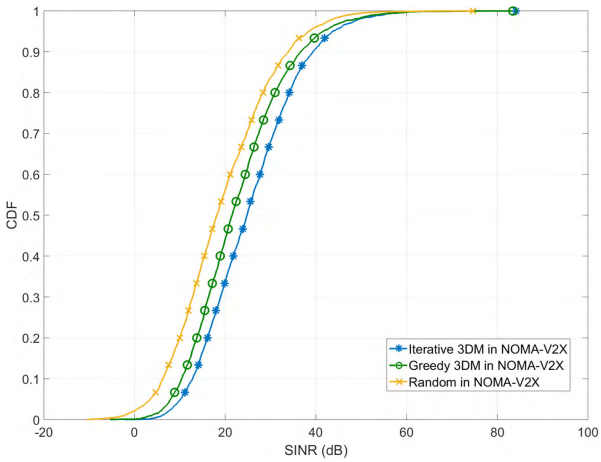

FIGURE 9. SINR CDF comparison with different algorithms.

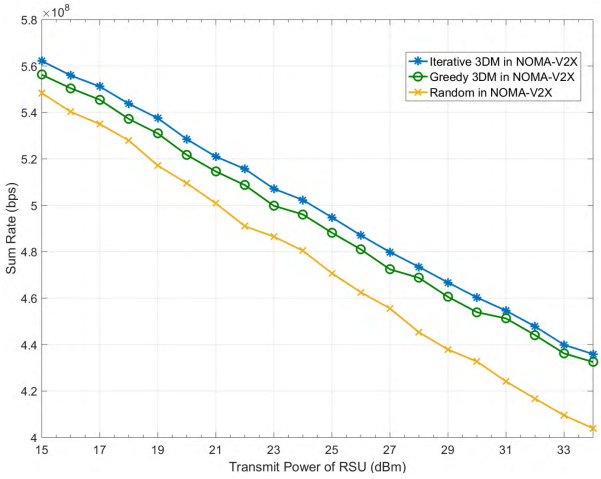

FIGURE 10. Sum rate comparison with different RSU transmit power.

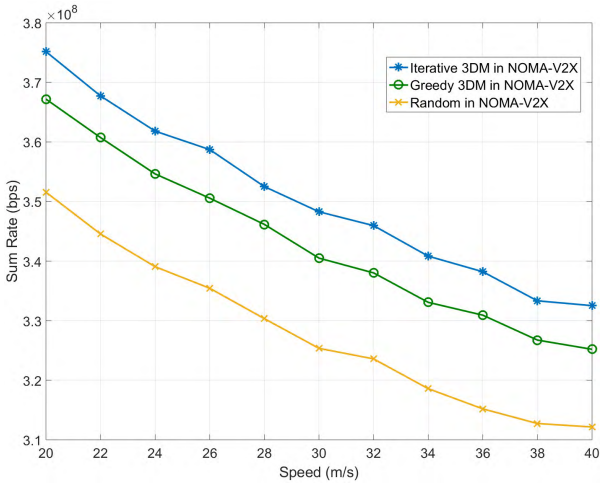

FIGURE 11. Sum rate comparison with different vehicle speed.

the same RB allocation algorithms as those of the scenario with NOMA in the scenario without NOMA. And we set the number of the vehicles in the case without NOMA as the same as that in the case with NOMA. The only difference between the case without NOMA and the case with NOMA is that all the previous receivers are considered to be independent users and assigned orthogonal RBs.

In Fig. 8, the cumulative distribution function (CDF) of the sum rate is compared among different algorithms for the NOMA-V2X scenario. Note that here the number of the vehicles is set as 42. The results here also indicate the performance advantages of our proposed iterative and greedy 3DM algorithms in NOMA-V2X networks. Then, we further compare the received SINR at the vehicles in V2I communications among different algorithms in Fig. 9, where the number of the vehicles is set as 42. We can see that the received SINR with the iterative 3DM algorithm is much higher than other algorithms, which verifies its good ability in interference control in such a complicated interference scenario. Both Fig. 8 and Fig. 9 indicate that our proposed IHG-3DM RB allocation protocol with the iterative 3DM algorithm can achieve a good network performance with low complexity in the NOMA-V2X networks.

Fig. 10 shows the sum rate performance comparison among different RB allocation algorithms under different RSU transmit power in the NOMA-V2X scenario. When the RSU transmit power increases, the sum rate of all the algorithms decreases accordingly. This is due to the interference level will be severer along with the increasing of the RSU transmit power, leading to heavier interference at the multi-V2V and uni-V2V receivers when sharing the same RB with a V2I communication group.

Then, we further investigate the impacts of the vehicle speed on different RB allocation algorithms in the NOMA-V2X scenario where the number of the vehicles is set as 42. The vehicle movement will impact the time-varying channel and the positions of the vehicles. With the same delay, the change of the channel state information and the vehicle positions compared with the reported ones cannot be ignored when the vehicles move fast, resulting in performance loss due to the outdated information effect. In Fig. 11, the network sum rate with different algorithms decreases with the increase

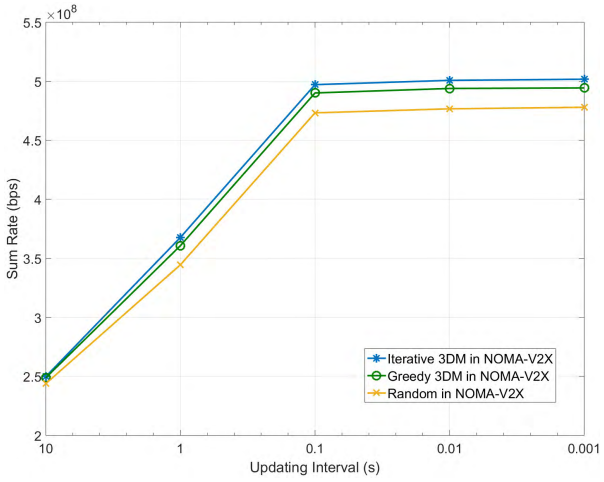

FIGURE 12. Sum rate comparison with different updating intervals.

of the vehicle speed. However, one should note that even in the high mobility cases, the performance of our proposed IHG-3DM RB allocation protocol with the iterative 3DM algorithm is still much better than that of the others.

In addition, we also simulate the performance under different updating intervals, using different RB allocation algorithms in the NOMA-V2X scenario. With a fixed vehicle speed (set as 25m/s in this simulation), a longer updating interval will also lead to larger difference between the real-time channel state and the reported one for the hypergraph construction. Fig. 12 indicates that, the sum rate first increases as the updating interval τ decreases. But the improvement in the sum rate becomes slow when the updating interval τ continues decreasing. This is because when the updating interval τ is small enough, the channel state will almost stay the same between neighboring updating periods, and thus the constructed hypergraph can well describe the current channel state and interference relationships. Therefore, further reducing the updating interval will not lead to obvious performance improvement.

V. CONCLUSIONS

In this paper, we investigated the resource allocation problem in NOMA-V2X networks, where both NOMA techniques and resource sharing based on spatial reuse are employed to improve the network performance. Then, a weighted 3-partite interference hypergraph was constructed to imitate the complex interference environment among all the V2X communication groups. With the help of our created 3-partite hypergraph, we put forward an IHG-3DM resource allocation protocol including a greedy 3DM algorithm and an iterative 3DM algorithm to solve the RB allocation problem. As a consequence, the network throughput was significantly improved with the help of our proposed IHG-3DM resource allocation protocol for the investigated NOMA-V2X communications, which was verified by the simulation results.

REFERENCES

[1] X. Cheng, C. Chen, W. Zhang, and Y. Yang, "5G-enabled cooperative intelligent vehicular (5GenCIV) framework: When benz meets marconi," *IEEE Intell. Syst.*, vol. 32, no. 3, pp. 53–59, May/Jun. 2017.

[2] S. Chen, J. Hu, Y. Shi, and L. Zhao, "LTE-V: A TD-LTE-based V2X solution for future vehicular network," *IEEE Internet Things J.*, vol. 3, no. 6, pp. 997–1005, Dec. 2016.

[3] X. Cheng, R. Zhang, and L. Yang, *5G-Enabled Vehicular Communications and Networking*. Cham, Switzerland: Springer, 2018.

[4] S. Chen, J. Hu, Y. Shi, Y. Peng, J. Fang, R. Zhao, and L. Zhao, "Vehicle-to-everything (v2x) services supported by LTE-based systems and 5G," *IEEE Commun. Standards Mag.*, vol. 1, no. 2, pp. 70–76, Jun. 2017.

[5] Q. Wei, L. Wang, Z. Feng, and Z. Ding, "Wireless resource management in LTE-U driven heterogeneous V2X communication networks," *IEEE Trans. Veh. Technol.*, vol. 67, no. 8, pp. 7508–7522, Aug. 2018.

[6] R. Hussain, J. Son, H. Eun, S. Kim, and H. Oh, "Rethinking vehicular communications: Merging VANET with cloud computing," in *Proc. IEEE 4th Int. Conf. Cloud Comput. Technol. Sci.*, Taipei, Taiwan, Dec. 2012, pp. 606–609.

[7] H. J. Qiu, I. W.-H. Ho, K. T. Chi, and Y. Xie, "A methodology for studying 802.11p VANET broadcasting performance with practical vehicle distribution," *IEEE Trans. Veh. Technol.*, vol. 64, no. 10, pp. 4756–4769, Sep. 2015.

[8] *IEEE Standard for Information Technology–Local and Metropolitan Area Networks–Specific Requirements–Part 11: Wireless LAN Medium Access Control (MAC) and Physical Layer (PHY) Specifications Amendment 6: Wireless Access in Vehicular Environments*, IEEE Standard 802.11p-2010, 2010.

[9] K. Doppler, M. Rinne, C. Wijting, C. B. Ribeiro, and K. Hugl, "Device-to-device communication as an underlay to LTE-advanced networks," *IEEE Commun. Mag.*, vol. 47, no. 12, pp. 42–49, Dec. 2009.

[10] R. Zhang, X. Cheng, L. Yang, and B. Jiao, "Interference graph-based resource allocation (InGRA) for D2D communications underlaying cellular networks," *IEEE Trans. Veh. Technol.*, vol. 64, no. 8, pp. 3844–3850, Aug. 2015.

[11] H. Tang and Z. Ding, "Mixed mode transmission and resource allocation for D2D communication," *IEEE Trans. Wireless Commun.*, vol. 15, no. 1, pp. 162–175, Jan. 2016.

[12] X. Cheng, L. Yang, and X. Shen, "D2D for intelligent transportation systems: A feasibility study," *IEEE Trans. Intell. Trans. Syst.*, vol. 16, no. 4, pp. 1784–1793, Jan. 2015.

[13] Z. Ding, X. Lei, G. K. Karagiannidis, R. Schober, J. Yuan, and V. Bhargava, "A survey on non-orthogonal multiple access for 5G networks: Research challenges and future trends," *IEEE J. Sel. Areas Commun.*, vol. 35, no. 10, pp. 2181–2195, Oct. 2017.

[14] L. Dai, B. Wang, Y. Yuan, S. Han, C.-L. I, and Z. Wang, "Non-orthogonal multiple access for 5G: Solutions, challenges, opportunities, and future research trends," *IEEE Commun. Mag.*, vol. 53, no. 9, pp. 74–81, Sep. 2015.

[15] Z. Ding, Z. Yang, P. Fan, and H. V. Poor, "On the performance of non-orthogonal multiple access in 5G systems with randomly deployed users," *IEEE Signal Process. Lett.*, vol. 21, no. 12, pp. 1501–1505, Dec. 2014.

[16] Z. Wu, K. Lu, C. Jiang, and X. Shao, "Comprehensive study and comparison on 5G NOMA schemes," *IEEE Access*, vol. 6, pp. 18511–18519, 2018.

[17] B. Di, L. Song, Y. Li, and Z. Han, "V2X meets NOMA: Non-orthogonal multiple access for 5G-enabled vehicular networks," *IEEE Wireless Commun.*, vol. 24, no. 6, pp. 14–21, Dec. 2017.

[18] L. Qian, Y. Wu, H. Zhou, and X. Shen, "Non-orthogonal multiple access vehicular small cell networks: Architecture and solution," *IEEE Netw.*, vol. 31, no. 4, pp. 15–21, Jul./Aug. 2017.

[19] S. Guo and X. Zhou, "Robust power allocation for NOMA in heterogeneous vehicular communications with imperfect channel estimation," in *Proc. IEEE 28th Annu. Int. Symp. Pers., Indoor, Mobile Radio Commun. (PIMRC)*, Montreal, QC, Canada, Oct. 2017, pp. 1–5.

[20] C. Chen, B. Wang, and R. Zhang, "Interference hypergraph-based resource allocation (IHG-RA) for NOMA-integrated V2X networks," *IEEE Internet Things J.*, vol. 6, no. 1, pp. 161–170, Feb. 2019.

[21] S. Sarkar and K. N. Sivarajan, "Hypergraph models for cellular mobile communication systems," *IEEE Trans. Veh. Technol.*, vol. 47, no. 2, pp. 460–471, May 1998.

[22] R. Zhang, X. Cheng, Q. Yao, C.-X. Wang, Y. Yang, and B. Jiao, "Interference graph-based resource-sharing schemes for vehicular networks," *IEEE Trans. Veh. Technol.*, vol. 62, no. 8, pp. 4028–4039, Oct. 2013.

[23] L. Yuan, J. Pan, N. Yang, Z. Ding, and J. Yuan, "Successive interference cancellation for LDPC coded nonorthogonal multiple access systems," *IEEE Trans. Veh. Technol.*, vol. 67, no. 6, pp. 5460–5464, Jun. 2018.
[24] B. Ling, C. Dong, J. Dai, and J. Lin, "Multiple decision aided successive interference cancellation receiver for NOMA systems," *IEEE Wireless Commun. Lett.*, vol. 6, no. 4, pp. 498–501, Aug. 2017.
[25] B. Chandra and M. M. Halldorsson, "Greedy local improvement and weighted set packing approximation," *J. Algorithms*, vol. 39, no. 2, pp. 223–240, May 2001.
[26] Y. H. Chan and L. C. Lau, "On linear and semidefinite programming relaxations for hypergraph matching," *Math. Program.*, vol. 135, nos. 1–2, pp. 123–148, Oct. 2012.
[27] L. Liang, S. Xie, G. Y. Li, Z. Ding, and X. Yu, "Graph-based resource sharing in vehicular communication," *IEEE Trans. Wireless Commun.*, vol. 17, no. 7, pp. 4579–4592, Jul. 2018.
[28] *Guidelines for Evaluation of Radio Interface Technologies for IMT-Advanced*, document Rep. ITU-R M.2135, 2008.
[29] H. Zheng, H. Li, S. Hou, and Z. Song, "Joint resource allocation with weighted max-min fairness for NOMA-enabled V2X communications," *IEEE Access*, vol. 6, pp. 65449–65462, 2018.
[30] H. W. Kuhn, "The Hungarian method for the assignment problem," *Naval Res. Logistics Quart.*, vol. 2, nos. 1–2, pp. 83–97, Mar. 1955.
[31] C. Guo, L. Liang, and G. Y. Li, "Resource allocation for low-latency vehicular communications: An effective capacity perspective," *IEEE J. Sel. Areas Commun.*, vol. 37, no. 4, pp. 905–917, Apr. 2019.

BAOJI WANG received the B.S. degree from Nankai University, Tianjin, China, in 2015. He is currently pursuing the Ph.D. degree with the State Key Laboratory of Advanced Optical Communication Systems and Networks, School of EECS, Peking University, Beijing, China.

His research interests include communication signal processing, vehicular communications and networking, and UAV communications. He received the Best Paper Awards at GLOBECOM'18.

RONGQING ZHANG (S'11–M'15) received the B.S. and Ph.D. degrees (Hons.) from Peking University, Beijing, China, in 2009 and 2014, respectively.

From 2014 to 2018, he was a Postdoctoral Research Fellow with Colorado State University, CO, USA. Since 2019, he has been an Associate Professor with Tongji University, Shanghai, China. He has authored or coauthored two books, two book chapters, and over 80 papers in refereed journals and conference proceedings. His current research interests include physical layer security, vehicular communications and networking, UAV communications, and autonomous driving. He was a recipient of the Academic Award for Excellent Doctoral Students, Ministry of Education of China, a co-recipient of the First-Class Natural Science Award, Ministry of Education of China, and received the Best Paper Awards at IEEE ITST'12, ICC'16, GLOBECOM'18, and ICC'19. He was also awarded the International Presidential Fellow of Colorado State University, in 2017. He is also serving as an Associate Editor for *IET Communications* and *Complexity* (Hindawi).

CHEN CHEN (S'07–M'09–SM'17) received the Ph.D. degree from Peking University, Beijing, China, in 2009, where he is currently an Associate Professor.

Since 2010, he has been a Principal Investigator of over ten funded research projects. His current research interests include the areas of signal processing, wireless communications, and networking. He has authored or coauthored over 50 journal papers, 30 conference papers, and two books in these areas. He was a recipient of two Outstanding Paper Awards from the Chinese Government of Beijing, the Best Paper Award at the IEEE ICNC'17, and a finalist of the Best Paper Award at the IEEE IWCMC'10 and Globecom'18. He has served as the Symposium Co-Chair, the Session Chair, and a Technical Program Committee Member for several international conferences.

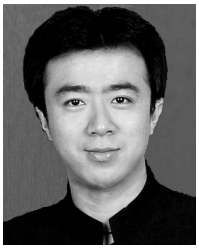

XIANG CHENG (S'05–M'10–SM'13) received the Ph.D. degree from Heriot-Watt University and The University of Edinburgh, Edinburgh, U.K., in 2009.

He is currently a Professor with Peking University. His general research interests include the areas of channel modeling and mobile communications, on which he has published more than 200 journal and conference papers, five books, and seven patents. He was a recipient of the IEEE Asia Pacific (AP) Outstanding Young Researcher Award, in 2015, and a co-recipient of the 2016 IEEE JSAC Best Paper Award: Leonard G. Abraham Prize, the NSFC Outstanding Young Investigator Award, and the First Rank and Second-Rand Awards in Natural Science of the Ministry of Education in China. He received the Best Paper Awards at IEEE ITST'12, ICCC'13, ITSC'14, ICC'16, ICNC'17, and GLOBECOM'18. He also received the Postgraduate Research Thesis Prize from The University of Edinburgh. He has served as the Symposium Leading-Chair, Co-Chair, and a Member of the Technical Program Committee for several international conferences. He is also an Associate Editor of the IEEE TRANSACTIONS ON INTELLIGENT TRANSPORTATION SYSTEMS and *Journal of Communications and Information Networks*. He is also an IEEE Distinguished Lecturer.

LIUQING YANG (S'02–M'04–SM'06–F'15) received the Ph.D. degree in electrical and computer engineering from the University of Minnesota, Minneapolis, in 2004.

She is currently a Professor with Colorado State University. Her general research interests include signal processing with applications to communications, networking, and power systems, on which she has published more than 310 journal and conference papers, four book chapters, and five books. She was a recipient of the ONR Young Investigator Program (YIP) Award, in 2007, the NSF Faculty Early Career Development (CAREER) Award, in 2009, and the Best Paper Award at the IEEE ICUWB'06, ICCC'13, ITSC'14, Globecom'14, ICC'16, WCSP'16, Globecom'18, ICCS'18, and ICC'19. She has served as an Associate/Senior Editor for the IEEE TRANSACTIONS ON COMMUNICATIONS, IEEE TRANSACTIONS ON WIRELESS COMMUNICATIONS, IEEE TRANSACTIONS ON SIGNAL PROCESSING, IEEE TRANSACTIONS ON INTELLIGENT TRANSPORTATION SYSTEMS, IEEE INTELLIGENT SYSTEMS, and *PHYCOM: Physical Communication*, as the Editor-in-Chief of the *IET Communications*, and as the Program Chair and Track/Symposium or TPC Chair for many conferences. She is also the Editor-in-Chief of the *IET Communications*.

YE JIN received the B.E and M.S. degrees from Peking University, China, in 1986 and 1989, respectively, where he is currently a Professor with the Institute of Modern Communications. His general research interests include the areas of satellite and wireless communications and networking. He was a recipient of the First Prize of the National Science and Technology Progress Awards of China. He has been a Principal Investigator of over 30 funded research projects.